



**DEPOSITION OF GRAPHENE-LIKE CARBON
ON COPPER FOIL USING METHANE**

by

**LEE HON CHEUN
(1531911670)**

A thesis submitted in fulfillment of the requirements for the degree of
Master of Science in Nanomaterial Engineering

**INSTITUTE OF NANO ELECTRONIC ENGINEERING
UNIVERSITI MALAYSIA PERLIS**

2017

UNIVERSITI MALAYSIA PERLIS (UniMAP)

DECLARATION OF THESIS

Author's full name : Lee Hon Cheun
Date of birth : 14/12/1990
Title : Deposition of graphene-like carbon on copper foil
using methane
Academic Session : 2015/2016

I hereby declare that the report becomes the property of Universiti Malaysia Perlis (UniMAP) and to be placed at the library of UniMAP. This report is classified as:

- CONFIDENTIAL** (Contains confidential information under the Official Secret Act 1972)
 RESTRICTED (Contains restricted information as specified by the organization where research was done)
 OPEN ACCESS I agree that my report is to be made immediately available as hard copy or on-line open access (full text)

I, the author, give permission to the UniMAP to reproduce this report in whole or in part for the purpose of research or academic exchange only (except during a period of _____ years, if so requested above).

Certified by:

SIGNATURE

SIGNATURE OF SUPERVISOR

901214015733
(NEW IC NO. / PASSPORT NO.)

DR. LIU WEI WEN
NAME OF SUPERVISOR

Date: _____

Date: _____

ACKNOWLEDGEMENT

From the depth of my heart, my wholehearted appreciation is forwarded to my main supervisor, Dr. Liu Wei Wen, for being an excellent mentor, taking precious time of his busy schedule to supervise my research and providing expert guidance and valuable comments throughout the years during the whole course of study. My sincere gratitude to Assoc. Professor Chai Siang Piao, my co-supervisor, for providing invaluable advice during my studies.

I would also like to thank Dr. Ruslinda A. Rahim, Director of Institute of Nano Electronic Engineering, Dr. Ramzan Mat Ayub, Deputy Director, Dr. Mohd Khairuddin Md Arshad and all the lecturers in this institute for their continuous motivation, precious support, guidance and shared their great knowledge in research throughout my studies these years. I extend my thanks to all the administrative staffs and laboratory technicians in Institute of Nano Electronic Engineering, for their assistance provided to me in achieving this project. All the personnel in Institute of Nano Electronic Engineering, are so helpful to assist me in accomplishing this project.

I am indeed very thankful to my dearest mother, Mdm. Gan Paik Kiow, and my brother, Lee Hon Ting who always on my side, giving their support to me, allowing me to pursue my studies. I also wish to dedicate this work in the memory of my beloved father, Mr. Lee Jia Huei, who passed away in the middle of my studies. His enduring sacrifice to enable me to have a better future will be always remembered.

I also wish to express my sincere gratitude and thanks to my friends and postgraduate students: Fatin Nabilah, Adzhri, Suhaimi, Iman, Shafiq Hafly, Faris, Zaki, Adelyn, Conlathan, Thivina, Khairun and others whom I am not able to address here. They have been helpful to provide their invaluable opinions, support and encouragement to me throughout whole course of study.

Last but not least, I want to thank Ministry of Education for providing me the financial support under Fundamental Research Grant Scheme (FRGS) (Project: A/C No: 9003-00415).

Thank you.

TABLE OF CONTENTS

	PAGE
DECLARATION OF THESIS	i
ACKNOWLEDGEMENT	ii
TABLE OF CONTENTS	iii
LIST OF FIGURES	vii
LIST OF TABLES	xii
LIST OF ABBREVIATIONS	xiii
LIST OF SYMBOLS	xv
ABSTRAK	xvi
ABSTRACT	xvii
Chapter 1 INTRODUCTION	
1.1. Catalysis	1
1.2. Allotropes of Carbon	2
1.3. Graphene	3
1.4. Natural Gas	5
1.5. Hydrogen	5
1.6. Methane Activation	6
1.7. Methane Decomposition	8
1.8. Problem Statement	9
1.9. Research Objectives	11
1.10. Scope of Study	11
1.11. Organization of the Thesis	12

Chapter 2 LITERATURE REVIEW

2.1.	History – Discovery of Graphene	14
2.2.	Structure of Graphene	15
2.3.	Synthesis of Graphene using Chemical Vapour Deposition (CVD)	16
2.3.1.	Solid Carbon Precursors	18
2.3.2.	Gas Carbon Precursors	22
2.3.3.	Liquid Carbon Precursors	26
2.4.	Characterization of Graphene	28
2.4.1.	Raman Spectroscopy	28
2.4.2.	X-ray Diffraction (XRD)	31
2.4.3.	X-ray Photoelectron (XPS)	33
2.4.4.	Scanning Electron Microscopy (SEM)/FESEM	37
2.5.	Growth Mechanism of Graphene Layer	47
2.5.1.	Differences between Surface Adsorption, and Segregation and Precipitation	47
2.5.2.	Copper Substrate	48
2.5.3.	Growth Mechanism of Multilayer Graphene	50
2.6.	Chemical Reaction from methane to graphene	56

Chapter 3 RESEARCH METHODOLOGY

3.1.	Overall Experimental Flowchart	58
3.2.	Selection of metal substrate	59
3.3.	Chemicals and Consumables	59
3.4.	Catalyst Activity Measurement	61
3.4.1.	Experimental Rig Setup	61
3.4.1(a)	Gas Mixing Segment	61

3.5.	Process Analysis of reaction parameters	63
3.6.	Catalyst and Graphene Characterization	65
3.6.1.	Raman Spectroscopy	65
3.6.2.	Scanning Electron Microscopy (SEM)	65
3.6.3.	Energy Dispersive X-ray (EDX)	66
3.6.4.	X-ray Photoelectron Spectroscopy (XPS)	66
3.6.5.	X-ray Diffraction (XRD)	66
Chapter 4 RESULTS & DISCUSSION		
4.1.	Effect of Reaction Times	67
4.2.	Effect of Reaction Temperatures	69
4.3.	Effect of Methane Flow Rates	71
4.4.	Comparison of Elemental Composition	73
4.5.	X-ray Diffraction Analysis	77
4.6.	X-ray Photoelectron Spectroscopy (XPS)	80
4.7.	Raman Analysis	85
4.8.	Effect of Oxygen in the Formation of Graphene-like Carbon Material	92
4.9.	Growth Mechanism of Graphene-like Carbon samples	93
Chapter 5 CONCLUSION		
5.1.	Conclusion	95
5.2.	Future Work and Recommendations	96
REFERENCES		99
APPENDIX A		109
APPENDIX B		110
APPENDIX C		113

©This item is protected by original copyright

LIST OF FIGURES

NO.		PAGE
1.1	Allotropes of carbon (Tiwari et al., 2016)	3
1.2	Structure of graphene (Jarosz, Skoda, Dudek, & Szukiewicz, 2016)	4
1.3	Schematic diagram of various methods for methane activation (T. V. Choudhary, Aksoylu, & Wayne Goodman, 2003)	8
2.1	(a) Lattice structure of graphene, (b) sp ² hybridization of carbon atoms to form the 2D crystal structure of graphene as well as delocalized π orbitals (X. Liang, 2014)	16
2.2	High magnification TEM image of the planar few-layer graphene film shown. The inset shows the intensity pattern along the line marked (Somani, Somani, & Umeno, 2006)	18
2.3	The schematic diagram of graphene flake growth process (Gan et al., 2012)	19
2.4	Raman spectra of the transferred graphene crystal checked randomly at four different areas. Raman spectra shows highly crystalline of a monolayer graphene (Sharma et al., 2014)	20
2.5	(a) The comparison of Raman spectra for graphene film synthesized by methanol, ethanol and 1-propanol (Guermoune et al., 2011). (b) Raman spectra of single (black and blue lines for 2-phenylethanol and ethanol, respectively), bi (green line), and tri (purple line) layer graphene (Campos-Delgado et al., 2013)	26
2.6	(a) Raman spectra of graphene and graphite (C. S. S. R. Kumar, 2012). (b) Raman spectra of CVD graphene and mechanically exfoliated graphene (Wan Li, Tan, Lowe, Abruña, & Ralph, 2011)	28
2.7	Evolution of the (a) G band, (b) G* band, (c) 2D band in the Raman spectra as functions of the number of graphene layers (Yoon et al., 2009)	30
2.8	(a) XRD plots for graphite, GO, graphene and FG (Naebe et al., 2015). (b) XRD patterns of natural graphite, GO and graphene (C. Wang et al., 2012)	32
2.9	XPS core level spectra (dots) obtained before and after 20 and 40s of hydrogen plasma exposure, respectively: (a), (b) and (c) CVD graphene on Cu and (d), (e) and (f) CVD graphene transferred onto SiO ₂	

	(300nm) on Si samples. The solid curves show the contributions of graphene and PMMA in each spectrum (Ferrah et al., 2016)	33
2.10	XPS analysis of graphene samples. XPS general spectra of (a) RGO-24 and RCMGO-24, (b) determination of K from K2p spectra of RCMGO-24, (c) C1s XPS spectra of RGO-24, and (d) C1s XPS spectra of RCMGO-24 (Rajagopalan & Chung, 2014)	35
2.11	(a) XPS spectrum of dried copper powder (Manukyan et al., 2014). (b) The XPS spectrum of Cu(2p) core level of the copper oxide nanostructures grown at NaOH concentration of 30mM (Akhavan, Azimirad, Safa, & Hasani, 2011)	36
2.12	FESEM images of thin graphene-like nanosheets in the upper liquid after centrifugation treatment. (a) Flat graphene film, (b, c) transparent graphene nanosheets, and (d) twisted and draped graphene (Chuan, 2013)	38
2.13	(a) Low-magnification, (b, c) moderate-magnification, (d) high-magnification FESEM images of few-layer graphene (Khai et al., 2013)	39
2.14	(a) FESEM image for the as-grown graphene films on copper, (b) High-magnification FESEM image of bilayer graphene sheet on copper grid, prepared by hot filament thermal chemical vapour deposition (Hawaladar et al., 2012). FESEM images of samples with graphene growth time of (c) 10 min, (d) 15 min (Dang, Che, Gao, Li, & Wang, 2014)	40
2.15	FESEM micrographs of graphene film transferred on (a) polished Si and (b) textured Si substrate and chemically prepared graphene film spin coated on (c) polished Si and (d) textured Si substrate (R. Kumar, Sharma, Bhatnagar, Mehta, & Rath, 2013)	41
2.16	(a) SEM image of a graphene sheet of 7 layers on a copper substrate. (b) SEM images of the graphene sheet of 7 layers transferred on a Si substrate, showing several wrinkles (Tu et al., 2014)	42
2.17	SEM micrographs of graphene grown on copper at 1070°C with 100 sccm H ₂ : (a) growth for 60s, (b) and (c) growth for 20s (Lisi et al., 2014)	43
2.18	SEM images contrast for different numbers of layers of graphene on polycrystalline nickel observed at (a) an elevated temperature during carbon segregation, (b) room temperature without exposure to air, and (c) room temperature after exposure to air (Takahashi, Yamada, Kato, Hibino, & Homma, 2012)	44
2.19	(a) SEM image (12µm × 9 µm) of a fully graphene covered surface, showing coherent graphene layer (Zeller, Dänhardt, Gsell, Schreck, & Wintterlin, 2012)	45

2.20	SEM images of CVD graphene on Cu. (a) 5ppm CH ₄ for 60 min. (b) 10ppm CH ₄ for 60min. (c) 20ppm CH ₄ for 30min. (d) 30ppm CH ₄ for 20min. Some are highlighted by dashed blue circles in images (c) and (d) are multilayer graphene domains (W. Wu et al., 2012)	46
2.21	Sketch of graphene formation by both direct chemisorption/deposition on Cu and precipitation/segregation on Ni (Losurdo, Giangregorio, Capezzuto, & Bruno, 2011)	47
2.22	Schematic diagrams of graphene growth mechanism on Cu surface (Y. Zhang, Zhang, & Zhou, 2013)	48
2.23	Graphene growth with separated isotopes by surface adsorption (X. Li, Cai, Colombo, et al., 2009)	49
2.24	The proposed mechanism for graphene domain growth. (a) Smooth Cu foil was obtained by cleaning in pre-treatment step. (b) Formation of large oxide nanoparticles on the pre-treated Cu foil. (c, d) in high hydrogen concentration condition, large single-crystal monolayer graphene was formed. (e, f) in low hydrogen condition, multilayer graphene was obtained (J. Liu et al., 2015)	50
2.25	Schematic of new bilayer graphene growth protocol. (a) Monolayer graphene is grown via standard CVD on Cu surface. (b) Carbon monomer intercalation occur via penetration mechanism. (c) Hydrogen gas is supplied to etch extra carbon species. (d) With desorption of hydrocarbons, high-quality bilayer graphene is obtained (P. Wu, Zhai, Li, & Yang, 2014)	51
2.26	The proposed model in (1) compared to model in (2) in terms of schematic side-view of substrate and multilayer configuration in which layer growth order, spatial arrangement and relative size are indicated (B. Wu et al., 2011)	52
2.27	Schematic of the experimental setup and the growth model for the graphene/Cu shell/core nanoparticles (Shiliang Wang et al., 2012)	53
2.28	Schematic illustration for the growth mechanism of graphene on polycrystalline Co film by radio frequency (RF) PECVD (Shumin Wang et al., 2013)	54
2.29	Schematic illustration of graphene domains growth on copper foil under the APCVD conditions: (a) nucleated graphene grain, (b) the size of graphene grain increases, (c) the second layer grows on the first layer epitaxially and (d) few-layer graphene produced by a multi-epitaxial growth (J. Zhang, Hu, Wang, & Wang, 2012)	55
3.1	Flowchart of overall experimental activities involved in this study	58

3.2	Schematic Diagram of the Experimental rig setup	60
3.3	Schematic diagram of reactor system	63
3.4	Copper foil in quartz boat	64
4.1	SEM images of carbon content for different reaction times of (a) 5 sec, (b) 30 sec, (c) 60 sec, (d) 90 sec and (e) 300 sec	68
4.2	SEM images of carbon content for different reaction temperatures of (a) 600°C, (b) 700°C, (c) 800°C, (d) 900°C and (e) 1050°C	70
4.3	SEM images of carbon content for different reaction methane flow rates of (a) 200mlpm, (b) 300mlpm, (c) 400mlpm, (d) 500mlpm and (e) 600mlpm	72
4.4	Comparison of carbon weight percentage on different reaction times	75
4.5	Comparison of carbon weight percentage on different reaction temperatures	76
4.6	Comparison of carbon weight percentage on different methane flow rates	76
4.7	XRD pattern of the samples prepared from the reaction times of 5 sec, 30sec, 60sec, 90sec and 300sec.	78
4.8	XRD patterns of the samples prepared from the reaction temperatures of 600°C, 700°C, 800°C, 900°C and 1050°C.	79
4.9	XRD patterns of samples prepared from the methane flow rates of 200, 300, 400, 500 and 600mlpm.	80
4.10	General scan for the as grown graphene-like on copper (G/Cu) using different methane flow rates of 200mlpm and 600mlpm, different reaction temperatures of 600°C and 1050°C and different reaction times of 5 seconds and 300 seconds	82
4.11	High-resolution XPS scan for C1s core level peak which consists of three components	83
4.12	High-resolution XPS scan for the O1s core level peak which was analysed into three components	84
4.13	High-resolution XPS scan for the Cu2p core level peak which contains several components	84
4.14	Raman spectrum of graphene. (C. S. S. R. Kumar, 2012)	86

4.15	Raman spectra for graphene-like samples grown using 5 seconds, 30 seconds, 60 seconds and 300 seconds	86
4.16	Raman spectra for graphene-like samples grown at temperatures of 600°C, 700°C, 800°C, 900°C and 1050°C	87
4.17	Raman spectra for graphene-like samples grown using methane flow rates of 200mlpm, 300mlpm, 400mlpm, 500mlpm and 600mlpm	87
4.18	Raman spectra of copper oxide (Akgul et al., 2014).	89
4.19	Raman spectra of synthesized graphene-like samples using different reaction times zooming at spectra region from 200-700 cm ⁻¹	89
4.20	Raman spectra of synthesized graphene-like samples using different reaction temperatures zooming at spectra region from 200-700 cm ⁻¹	90
4.21	Raman spectra of synthesized graphene-like samples using different methane flow rate zooming at spectra region from 200-700 cm ⁻¹	90
4.22	Raman spectrum of synthesized graphene-like samples at 200-700 cm ⁻¹	91
A.1	XRD pattern of sample prepared from the reaction time of 5 seconds	110
A.2	XRD pattern of sample prepared from the reaction time of 300 seconds	111
A.3	XRD pattern of bare copper foil	112

LIST OF TABLES

NO.		PAGE
1.1	Typical composition of natural gas (Abu Bakar & Ali, 2010)	5
3.1	Table of chemicals and reagents	59
3.2	Primary elements in the experimental rig and their roles	61
3.3	Different reaction times are varied	64
3.4	Different reaction temperatures are varied	64
3.5	Different reaction flow rates are varied	65
4.1	Elemental compositions of samples synthesized using different reaction times.	69
4.2	Elemental compositions of samples synthesized using different reaction temperatures	71
4.3	Elemental compositions of samples synthesized using different methane flow rates.	73

LIST OF ABBREVIATIONS

0-D	Zero dimension
1-D	One dimension
2-D	Two dimension
3-D	Three dimension
CDM	Catalytic decomposition of methane
CNFs	Carbon nanofibers
CNTs	Carbon Nanotubes
CNWs	Carbon Nanowalls
CVD	Chemical Vapour Deposition
DFT	Density Functional Theory
EDX	Energy Dispersive X-ray
FESEM	Field Emission Scanning Electron Microscopy
FG	Functionalized graphene
GO	Graphene Oxide
HOPG	Highly Oriented Pyrolytic Graphite
ICPCVD	Inductively Coupled Plasma Enhanced Chemical Vapour Deposition
MPCVD	Microwave Plasma Chemical Vapour Deposition
OCM	Oxidative coupling of methane
PECVD	Plasma Enhanced Chemical Vapour Deposition
PMMA	Poly(methyl methacrylate)
POM	Oxidation of methane
RCMGO	Reduced Chemically Modified Graphene Oxide
RF	Radio Frequency
RGO	Reduced Graphene Oxide
SEM	Scanning Electron Microscopy
SRM	Steam Reforming of methane
Syngas	Synthesis gas

TDM	Thermal Decomposition of methane
TEM	Transmission Electron Microscopy
TRG	Thermally Reduced Graphene
UHV-CVD	Ultra-high Vacuum Chemical Vapour Deposition
XPS	X-ray Photoelectron Spectroscopy
XRD	X-ray Diffraction

©This item is protected by original copyright

LIST OF SYMBOLS

Π	Pi
Ar	Argon
Å	Angstrom
CH ₄	Methane
C ₂ H ₄	Ethylene
C ₂ H ₆	Ethane
C ₃ H ₈	Propane
C ₄ H ₁₀	Butane
C ₁₂ H ₂₂ O ₁₁	Sucrose
C ₁₃ H ₁₀	Fluorene
CO ₂	Carbon Dioxide
Cu	Copper
CuO	Cupric oxide
Cu ₂ O	Cuprous oxide
H ₂	Hydrogen
H ₂ S	Hydrogen sulphide
HCB	Hexachlorobenzene
He	Helium
mlpm	Milli liter per minute
N ₂	Nitrogen
Ne	Neon
Ni	Nickel
O ₂	Oxygen
Pt	Platinum
Si	Silicon
Xe	Xenon

Pemendapan Karbon seperti Graphene pada Kerajang Kumprum menggunakan Metana

ABSTRAK

Graphene, allotrope karbon dua dimensi yang terdiri daripada satu lapisan atom karbon hibrid sp^2 yang disusun dalam konfigurasi heksagon. Sejak graphene ditemui pada tahun 2004, penyelidikan graphene telah meningkat dengan pesat kerana sifatnya yang unik dan luar biasa. Pelbagai kaedah telah dicadangkan untuk mensintesis lapisan graphene di mana kaedah yang paling menjanjikan adalah penggunaan pemendapan wap kimia (CVD). Walau bagaimanapun, masih terdapat banyak masalah mengenai kesan parameter tindak balas dan mekanisme pertumbuhan dalam pertumbuhan pemangkin menggunakan kaedah CVD. Contohnya, pemisahan lapisan graphene daripada substrat dan keseragaman lapisan graphene pada substrat. Dalam kajian ini, penguraian pemangkin metana digunakan untuk menghasilkan lapisan graphene pada kerajang kuprum. Parameter tindak balas dalam proses CVD termasuk tempoh masa, suhu tindak balas dan kadar aliran metana telah diubah untuk mengkaji kesan parameter ini pada sampel graphene. Pelbagai ujian pencirian termasuk Kemikroskopan Elektron Imbasan (SEM), Kemikroskopan Sinar-X Dispersive Tenaga (EDX), Belauan Sinar-X (XRD), Kemikroskopan Raman dan Kemikroskopan Foelektron Sinar-X (XPS) telah dijalankan pada sampel graphene yang dihasilkan. Aglomerasi karbon dapat dikesan di sempadan butiran substrat kuprum. Kandungan karbon pada sampel graphene meningkat apabila tempoh masa, suhu tindak balas atau kadar aliran metana meningkat. Ini menunjukkan bahawa lebih banyak atom karbon telah didepositkan pada kerajang kuprum apabila tempoh masa, suhu tindak balas dan kadar aliran metana meningkat. Sebaliknya, peratusan berat aglomerasi karbon di sempadan butiran adalah lebih tinggi daripada pusat butiran dalam semua sampel. Selain itu, keputusan XRD menunjukkan kehadiran puncak pembelauan untuk kuprum-oksida dan puncak grafit kecil pada $2\theta=26.5^\circ$ yang menandakan pembentukan karbon seperti graphene dengan kuantiti yang sangat rendah di bawah masa reaksi tinggi (90 and 300 saat), suhu reaksi tinggi (1050°C) dan kadar aliran metana (200-600mlpm). Di samping itu, keputusan XPS mengesahkan kehadiran spektrum C1s pada 284.8eV yang berasaskan kewujudan karbon hibrid sp^2 pada sampel. Dengan karbon hibrid sp^2 ini, dipercayai bahawa jumlah struktur seperti graphene yang sangat rendah telah disintesis yang diedarkan secara rawak di permukaan sampel kami. Walau bagaimanapun, tiada puncak Raman di D (1350cm^{-1}), G (1580cm^{-1}) dan 2D (2700cm^{-1}) dijumpai dengan menunjukkan tiada graphene pada sampel tetapi hanya puncak Raman kuprum-oksida dapat dikesan. Daripada keputusan di atas, sampel yang dihasilkan mengandungi lapisan graphene dalam kuantiti yang sangat kecil disebabkan dua batasan: tiada gas hidrogen dan kadar aliran metana yang tinggi telah digunakan. Tambahan pula, kehadiran spesies oksigen di dalam relau CVD telah menghalang pembentukan lapisan graphene dan akhirnya, pembentukan lapisan graphene tidak digalakkan pada substrat kuprum.

Deposition of Graphene-like Carbon on Copper Foil using Methane

ABSTRACT

Graphene, a two-dimensional carbon allotrope that is made up of single-layer sp^2 hybridized carbon atoms arranged in a hexagonal configuration. Since graphene was discovered in year 2004, graphene research has surged exponentially owing to its unique and remarkable properties. A variety of methods have been proposed to synthesize graphene layer of which the most promising method is using chemical vapour deposition (CVD). However, there still lie a lot of issues about effects of reaction parameters and growth mechanism in the catalytic growth using CVD method. For example, is the separation of the graphene from the substrate and uniformity of graphene layer on the substrate. In this study, catalytic decomposition of methane was employed for producing graphene layer on copper foil. The reaction parameters in CVD process including reaction times, reaction temperatures and methane flow rates were varied to study the impact of these parameters on the graphene samples. Various characterization tests including Scanning Electron Microscopy (SEM), Energy Dispersive X-ray (EDX), X-ray diffraction (XRD), Raman spectroscopy and X-ray photoelectron spectroscopy (XPS) were carried out on the graphene samples produced. The agglomerations of carbon were observed at the grain boundaries of the copper substrate. The carbon content on the graphene sample increased when the reaction time, reaction temperature or methane flow rate were increased. This indicated that more and more carbon atoms were deposited on the copper foil when the reaction time, reaction temperature and methane flow rate were increased. On the other hand, the weight percentage of carbon agglomeration at the grain boundaries was higher than that of the centre of grains in all samples. Besides, XRD diffraction peak for the copper oxide and small graphite peak at $2\theta=26.5^\circ$ were seen which signified very low quantity of graphene-like carbon structures were formed under high reaction times (90 and 300 seconds), high reaction temperature (1050°C) and methane flow rates (200-600mlpm). In addition, XPS results confirmed the presence of the C1s spectrum at 284.8eV which ascribed to the existence of sp^2 -hybridized carbon on the samples. With this sp^2 -hybridized carbon, it is confirmed again very low amount of graphene-like carbon materials were synthesized and distributed randomly on the surface of our samples. However, no Raman peak at D(1350cm^{-1}), G(1580cm^{-1}) and 2D(2700cm^{-1}) were shown to represent the graphene on the sample but only the Raman peaks of copper oxide were detected. From above results, the produced samples contain very small amount of graphene layer due to two limitations: no hydrogen gas and high methane flow rate were used. Furthermore, the presence of oxygen species in the CVD furnace even further hinders the formation of graphene layer and eventually, the graphene layer was less likely to be formed on the copper substrate.

CHAPTER 1

INTRODUCTION

1.1. Catalysis

The term 'catalysis' elucidates the chemical reaction is influenced due to the participation of the additional material in the chemical reaction (Berzelius, 1836). The material with the said property is called catalyst which can greatly modify the rate of attainment of chemical equilibrium and maintain its original form. In general, catalysts can be divided into three main types, those are: heterogenous catalysts, homogenous catalysts and biocatalysts or enzymes.

Heterogenous catalysts are different from homogenous catalysts by the phases of the catalysts during the reaction. Heterogenous catalysts could exist in different phases, usually solid, as compared to reactants and products. Heterogenous catalysts are crucial in manufacturing and research fields as they were used in vast variety of chemical processes. For instance, catalytic cracking, production of acids, catalytic reforming, and hydrogenation.

In contrast, homogeneous catalysts are catalysts that are in the same phase as the reactants and products. There are some examples of heterogeneous catalysis: Lewis acids as homogeneous catalyst, general acid and base catalysis and porphyrin complexes (Van Leeuwen, 2004). By comparing heterogeneous and homogeneous catalysts, the former is usually more stable and slower in the degradation of the latter (Spessard & Miessler, 2010).

On the other hand, biocatalysts or enzymes are normally natural proteins that are produced by living organisms and they are used to perform chemical transformation on organic compounds. Biocatalysts are imperative to life because they speed up metabolic

reactions to a very tremendous extent, without undergo any change in the biocatalysts in the process. Biocatalysts show some distinct advantages, such as, high specificity, highly biodegradable, high activity under moderate conditions, and are treated as natural products. However, biocatalysts are complex in molecular structures and costly in production costs are the definite disadvantages of the enzymes (Illanes, 2008).

Copper foil is commonly used as the metal catalyst to synthesize graphene films (X. Li, Colombo, & Ruoff, 2016) due to its low carbon solubility (Froumin, Frage, Aizenshtein, & Dariel, 2003). The catalytic activity of copper foil during the CVD is to facilitate the decomposition of carbon precursor and nucleation of graphene lattice (Mattevi, Kim, & Chhowalla, 2011). CVD is also one of the common methods to produce graphene film. Via CVD, the gas precursors react and decompose to adsorb on the surface of the substrate to produce the desired deposit which is graphene layer. Owing to the low carbon solubility in copper, the dominant growth mechanism of graphene on copper is surface adsorption, unlike the segregation and precipitation growth mechanism in high carbon solubility catalyst (X. Li, Cai, Colombo, & Ruoff, 2009).

1.2. Allotropes of Carbon

Allotropy is the attribute of elements to exist in two or more different forms in the same physical states. These allotropes are simply different in the structural configurations where the atoms are associated in different manner. However, allotropy only occurs with certain elements. In previous years, diamond and graphite are the only known allotropes of carbon until the discovery of fullerene in year 1985 (Kroto, Heath, O'Brien, Curl, & Smalley, 1985) and carbon nanotubes (CNTs) in year 1991 (Iijima, 1991). In year 2004, the discovery of graphene has further added to the existed allotropes of carbon.

Carbon atom consists of six electrons, which fill in the atomic orbitals of $1s^2$, $2s^2$ and $2p^2$. Thus, the electrons in the orbitals provide three viable hybridizations in carbon bonding, they are: sp , sp^2 and sp^3 hybridization configurations. Carbon hybridization bonding by sp configuration results in chain structures, sp^2 bonding gives rise to planar structures and sp^3 hybridization produces tetrahedral structures. Therefore, the formation of different allotropes of carbon owes to the different hybridizations in carbon bonding. Figure 1.1. shows a few allotropes of carbon and their atoms arrangement. For instance, diamond is formed where the carbon atoms are connected in a tetrahedral structure, graphite is made up of carbon atoms in sheets of hexagonal lattice and graphene consists of single sheet of graphite layer.

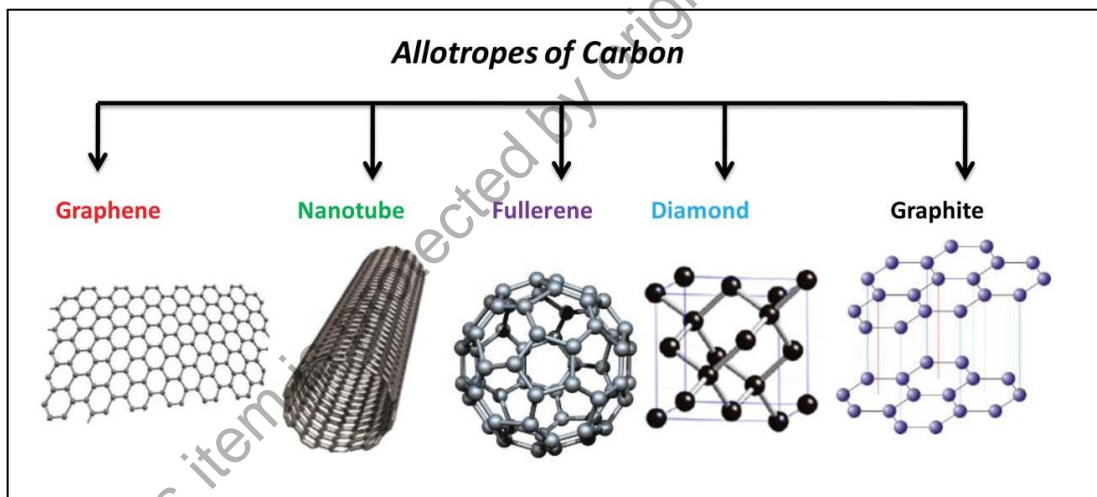


Figure 1.1: Allotropes of carbon (Tiwari et al., 2016).

1.3. Graphene

Graphene is a two-dimensional (2D) material found to be thermodynamically stable in nature. It was thought to be an impossible material to exist until two great scientists, Andrei Geim and Kostya Novoselov isolated graphene layer via a rather simple technique, by regular scotch tape (Novoselov et al., 2004). Since then, the graphene research has developed quickly due to graphene possesses peculiar properties. The

extraordinary attributes have intrigued the interest of many researchers and scientists from all over the world and thus, it emerged to be a popular chapter in research field thereafter. The remarkable properties of graphene also show prospect to be used in several promising applications. For example, graphene can be applied in transparent conductive electrodes and photovoltaic cells due to its high optical transparency and high electrical conductivity.

As the simplest allotrope of carbon, graphene is made up of single two-dimensional carbon atoms arranged in hexagonal honeycomb lattice as shown in Figure 1.2. Graphene is the basic building block of other carbon allotropes. For instance, graphene can be wrapped up into fullerene (0-D), rolled up into carbon nanotube (1-D), and stacked up into many layers graphite (3-D). Due to its simplicity and one atom thick, it is the thinnest material known to man and has almost zero mass. Besides, its electrical conductivity of six orders of magnitude is higher than copper, flexible yet harder than diamond and optical transparent. The full potential of graphene will be explored and effectively be utilized by researchers and industrialists in the near future.

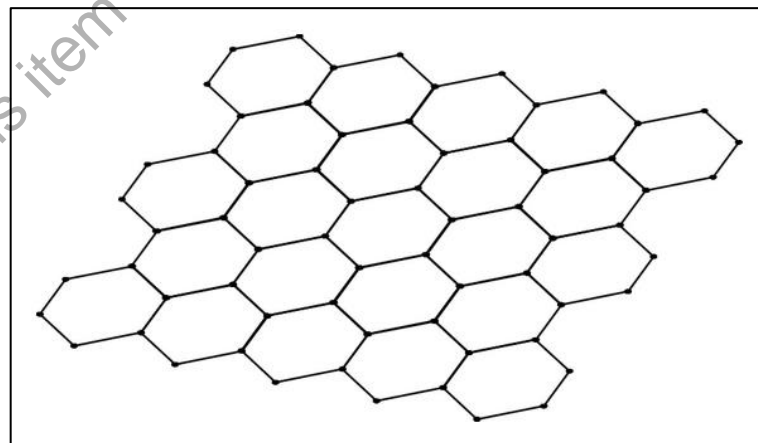


Figure 1.2: Structure of graphene (Jarosz, Skoda, Dudek, & Szukiewicz, 2016).

1.4. Natural Gas

Natural gas is generally considered a non-renewable fossil fuel which is found deep beneath the earth's surface. Natural gas is formed when decomposed plants and animals are exposed to extremely high geological stresses which transformed the organic compounds into natural gas. The transformation process is believed to take millions of years to happen. Natural gas contains a mixture of hydrocarbon gas that are made up mostly of methane, and also including minor amounts of other alkanes. The typical composition of natural gas is shown in Table 1. Natural gas is combustible and it gives off energy when it is burned. However, unlike other fossil fuels, natural gas is comparably cleaner during combustion and emits lower levels of harmful substances into the surroundings. Applications of natural gas is very broad in diversity, in which there are wide variety of ways to convert natural gas into value-added products, such as CNTs, graphene, and other carbon materials. Conversion of natural gas is usually expressed as methane conversion because methane is the primary component of natural gas (70-90%).

Table 1.1: Typical composition of natural gas (Abu Bakar & Ali, 2010).

Chemical Name	Chemical Formula	Percentage (%)
Methane	CH ₄	70-90%
Ethane	C ₂ H ₆	0-20%
Propane	C ₃ H ₈	
Butane	C ₄ H ₁₀	
Carbon Dioxide	CO ₂	0-8%
Oxygen	O ₂	0-0.02%
Nitrogen	N ₂	0-5%
Hydrogen sulphide	H ₂ S	0-5%
Rare gases	Ar, He, Ne, Xe	Trace

1.5. Hydrogen

By viewing the problems of the future shortage supply of petroleum and the upsurge of the prices of petroleum-based fuels, the shifting of the supply of energy towards the alternative fuels sector has been concerned since many years ago. Moreover,

the rising of the awareness of the greenhouse gas emissions has further increased the pace to move to another different source of fuels for energy. Consequently, it can be observed from Figure 1.3 that approximately half of the energy consumption globally by the end of the 21st century. This indicates that the shifting of the energy consumption to hydrogen as the alternative energy source is one of the choices for consideration by mankind. On the other hand, hydrogen gas is one of the important gases to be used to synthesize CNTs and graphene in chemical vapor deposition (CVD).

1.6. Methane Activation

Effective implementation of methane for various applications remains to be one of the continuing issues in catalysis. A wide variety of approaches including direct and indirect ways, have been developed for the conversion of methane to more valuable products. Figure 1.4 shows different approaches for methane activation. Oxidative coupling of methane (OCM) became prominent topics in methane activation research after Keller and Bhasin (1982) reported the direct conversion of methane into ethylene for the first time in year 1982. The reason to the fact that OCM became prominent is that OCM offers a cheaper and simpler path for higher hydrocarbon production from methane as compared with hydrocarbon produced by synthesis gas (syngas) approach.

This is followed by reforming of methane to synthesis gas (syngas) which can be carried out by a few methods, as shown in Figure 1.4, i.e. steam reforming of methane (SRM), partial oxidation of methane (POM), and CO₂ reforming of methane. These three reforming processes produce syngas with different CO/H₂ ratios, namely 1:3, 1:2 and 1:1. SRM processes methane at high temperature in a reformer in the presence of metal-based catalyst such as nickel. In addition, SRM represents the current trend for hydrogen

production due to methane has the highest H/C ratio which can yield more hydrogen than others (P. Tang, Zhu, Wu, & Ma, 2014). On the other hand, POM process also requires high temperatures (1100 – 1200 K) to obtain the CO₂ and H₂, whereas POM has safety issue to industrial application due to the reaction is difficult to be controlled and would end up in local overheating. Lastly, CO₂ reforming of methane consumes two greenhouse gases (CO₂ and CH₄) and transforms them into valuable syngas. This process provides an effective way to employ low grade natural gases and reduces emission of CO₂ and CH₄ into the atmosphere. Furthermore, the syngas produced can be further processed into methanol which is favorable to be used in production of gasoline. The Fischer-Tropsch process (Vannice, 1976) is another alternative option to process syngas by converting syngas into hydrocarbon.

In addition, direct methane decomposition produces only H₂ and solid carbon without the addition of other substances like the reforming processes which were mentioned above. The carbon byproduct generated from the methane decomposition process is beneficial as they contain different types of valuable carbon, including CNTs, carbon black and graphene.